Sonochemical Synthesis of Functionalized Amorphous Iron Oxide Nanoparticles

Kurikka V. P. M. Shafi,[†,§] Abraham Ulman,*[,†,§] Xingzhong Yan,[‡,§] Nan-Loh Yang,[‡,§] Claude Estournès,[∥] Henry White,[§,⊥] and Miriam Rafailovich[§,⊥]

Department of Chemical Engineering and Chemistry, Polytechnic University, Brooklyn, New York 11201, Department of Chemistry, CUNY at Staten Island, 2800 Victory Blvd, Staten Island, New York 10314, The NSF MRSEC for Polymers at Engineered Interfaces, Institut de Physique et Chimie des Matériaux de Strasbourg, Groupe des Matériaux Inorganiques, 23 rue du Loess, 67037 Strasbourg Cedex, France, and Department of Materials Sciences and Engineering, State University of New York at Stony Brook, Stony Brook, New York 11794-2275

Received March 21, 2001. In Final Form: June 4, 2001

Sonochemical decomposition of $Fe(CO)_5$ was carried out in the presence of different surfactants. The reactions give stable colloids of undecenoate, dodecyl sulfonate, and octyl phosphonate coated Fe_2O_3 nanoparticles of 5−16 nm in diameter. The ionic binding of the surfactants to the nanoparticle surfaces was confirmed by FTIR spectroscopy. Electron paramagnetic resonance measurements, magnetization curves, and zero-field cooled and field cooled studies indicate that the as-prepared amorphous nanoparticles are superparamagnetic. These studies show that the phosphonate-coated nanoparticles behave in a strikingly different manner from the other particles. It is proposed that the extra negative charge on the phosphonate, as compared to the carboxylate and sulfonate groups, makes it a strong bridging bidentate ligand, resulting in the formation of strong ionic bonds to the *surface* Fe^{3+} ions, which decreases the number of unpaired spins, possibly through a double superexchange mechanism through a $Fe^{3+}-O-P-O-Fe^{3+}$ pathway.

Confinement and quantum size effects in nanoparticles induce properties that are significantly different from those of the bulk material due to their reduced dimensions. Such properties are of technological importance and of current research interest.[1] Magnetic nanoparticles have a wide range of applications in, for example, information storage,[2] color imaging,[3] magnetic refrigeration,[4] ferrofluids,[5] cell sorting,[6] medical diagnosis,[7] and controlled drug delivery.[8] However, there have been relatively few studies on magnetic nanoparticles compared to, say, semiconductor nanoparticles. Various methods have been reported for the synthesis of metal oxide nanoparticles, such as flame pyrolysis,[9] sol−gel reactions,[10] and chemical oxidation in micellar media or in polymer or mineral matrixes.[11] In general, these methods do not yield pure amorphous phases, and good control of particle size and achievement of monodispersity (i.e., narrow size distribution) are still the challenges in all these techniques.

Amorphous materials have many important applications in magneto-optical devices such as optical isolators, optical switches, and so forth.[12] In sonochemistry, the acoustic cavitation, that is, the formation, growth, and implosive collapse of a bubble in an irradiated liquid, generates a transient localized hot spot, with an effective temperature of 5000 K and a nanosecond lifetime.[13] The rapid cavitational cooling rate ($\geq 10^{10}$ K s^{-1}) is much greater than that obtained by the conventional melt-spinning technique, normally used for the preparation of metallic glasses (10^5-10^6 K s^{-1}),[14] thus ideal for preparing amorphous materials.

The advantage of sonochemistry is that one can obtain atomic level mixing of the constituent ions in the amorphous phase so that the crystalline phase can be obtained by annealing at relatively low temperatures. The cavitation is a quenching process, and hence the composition of the particles formed is identical to the composition of the vapor in the bubbles, without phase separation. This becomes important in the preparation of crystalline ferrite or other mixed oxide materials where the conventional ceramic method requires heating at high temperatures, which can lead to the increase in particle size and aggregation. Sonochemistry had been used to prepare various kinds of nanostructured amorphous magnetic materials of metal,[15] metal alloy,[16] oxide,[17] ferrite,[18] and nitride.[19]

* To whom correspondence should be addressed. Phone: (718) 260-3119. Fax: (718) 260-3125. E-fax: (810) 277-6217. E-mail: aulman@poly.edu.

† Polytechnic University.

‡ CUNY at Staten Island.

§ The NSF MRSEC for Polymers at Engineered Interfaces.

∥ Institut de Physique et Chimie des Matériaux de Strasbourg.

⊥ State University of New York at Stony Brook.

(1) (a) Ozin, G. A. *Adv. Mater.* **1992**, *4*, 612. (b) Gleiter, H. *Adv. Mater.* **1992**, *4*, 474.

(2) Audram, R. G.; Huguenard, A. P. U.S. Patent 4,302,523, 1981.

(3) Ziolo, R. F. U.S. Patent 4,474,866, 1984.

(4) McMichael, R. D.; Shull, R. D.; Swartzendruber, L. J.; Bennett, L. H.; Watson, R. E. *J. Magn. Magn. Mater.* **1992**, *111*, 29.

(5) Rosensweig, R. E. *Ferrohydrodynamics*; MIT Press: Cambridge, 1985.

(6) Pope, N. M.; Alsop, R. C.; Chang, Y.-A.; Sonith, A. K. *J. Biomed. Mater. Res.* **1994**, *28*, 449.

(7) Marchessault, R. H.; Richard, S.; Rioux, P. *Carbohydr. Res.* **1992**, *224*, 133.

(8) Bhatnagar, S. P.; Rosensweig, R. E. *J. Magn. Magn. Mater.* **1995**, *149*, 198.

(9) Grimm, S.; Schultz, M.; Barth, S.; Müller, R. *J. Mater. Sci.* **1997**, *32*, 1083.

(10) (a) Stöber, W.; Fink, A.; Böhn, E. *J. Colloid Interface Sci.* **1968**, *26*, 62. (b) Jean, J. H.; Ring, T. A. *Langmuir* **1986**, *2*, 251.

(11) Mounien, N.; Pileni, M. P. *Chem. Mater.* **1996**, *8*, 1128.

(12) Kommareddi, N. S.; Tata, M.; John, V. T.; McPherson, G. L.; Herman, M. F.; Lee, Y.-S.; O'Connor, C. J.; Akkara, J. A.; Kaplan, D. L. *Chem. Mater.* **1996**, *8*, 801.

(13) (a) Suslick, K. S. *Science* **1990**, *247*, 1439. (b) Flint, E. B.; Suslick, K. S. *Science*, **1991**, *253*, 1397. (c) Atchley, A. A.; Crum, L. A. In *Ultrasound, its Chemical, Physical and Biological Effect*; Suslick, K. S., Ed.; VCH Press: New York, 1988.

(14) Greer, A. L. *Science* **1995**, *267*, 1947.

10.1021/la010421+ CCC: $20.00
Published on Web 07/12/2001

Amorphous iron oxide nanoparticles have served as substrates for the self-assembly of thiols,[20] alcohols,[21] carboxylic acids,[22] octadecyltrichlorosilane (OTS), and sodium dodecyl sulfate (SDS).[23] However, in all these cases coating was accomplished ex situ, that is, the nanoparticles were prepared first (sonochemically) and then subjected to the surfactant solution under agitation. By use of long-chain surfactants, such as lauric acid and oleic acid, poly(vinyl) amine and double surfactant layers, the size of particles can be controlled and their aggregation can be prevented. The role of surfactant is to produce the entropic repulsion needed to overcome the short-range van der Waals attraction that otherwise results in irreversible particle aggregation.

In the sonochemical approach presented here, efficient coating of the nanoparticles might be achieved by preparing the amorphous nanoparticles by sonochemical decomposition of volatile precursors in the presence of suitable surfactants.[24,25] Because of the extreme reaction conditions associated with the cavitation process, there was a question of whether organic surfactants would survive the sonochemical decomposition. However, one can assume that due to the low vapor pressure of these polar molecules, the collapsing bubbles will contain mainly, if not exclusively, the volatile $Fe(CO)_5$. In that case, the ratio of $Fe(CO)_5$ to surfactant may control the resulting size and size distribution of the oxide nanoparticle. In this paper, we describe results of such experiments, where sonochemical decomposition of $Fe(CO)_5$ was carried out in the presence of different surfactants.

The magnetic colloids of iron oxides were prepared by ultrasonic decomposition of the volatile precursor ($Fe(CO)_5$) solution in decane (Aldrich, anhydrous), using a high-intensity ultrasonic probe, with the surfactants 11-undecenoic acid ($CH_2{=}CH(CH_2)_8COOH$, Aldrich), dodecyl sulfonic acid ($C_{12}H_{23}SO_3H$, Alfa), and octyl phosphonic acid ($C_8H_{17}PO_3H_2$, Alfa) as stabilizing agents. Thus, a decane solution of 0.5 M $Fe(CO)_5$ and 0.05 M surfactants was sonicated at 273 K for 3 h, under air atmosphere, using a high-intensity ultrasonic probe (Sonics, model VC 601, 1.25 cm Ti horn, 20 kHz, 100 W/cm^2). The resulting black solution was evacuated to remove any unreacted $Fe(CO)_5$. The colloidal solution thus obtained was stable for more than 3 months, at ambient conditions.

Transmission electron microscopy (TEM) images were obtained by placing one or two drops of the colloidal solution onto a carbon-stabilized Formvar-coated copper grid (200 mesh) and drying it. Alternatively, the functionalized nanoparticles were floated at the air−water interface of a Langmuir trough and transferred to a copper grid. Samples for FTIR analysis were prepared by mixing the evaporated residue of the colloids with spectroscopic grade KBr in the ratio 1:50. Spectra were recorded, using samples of equal weight, on a Nicolet 760 spectrophotometer equipped with a He−Ne laser and an MCT detector, in 2 cm^{-1} resolution.

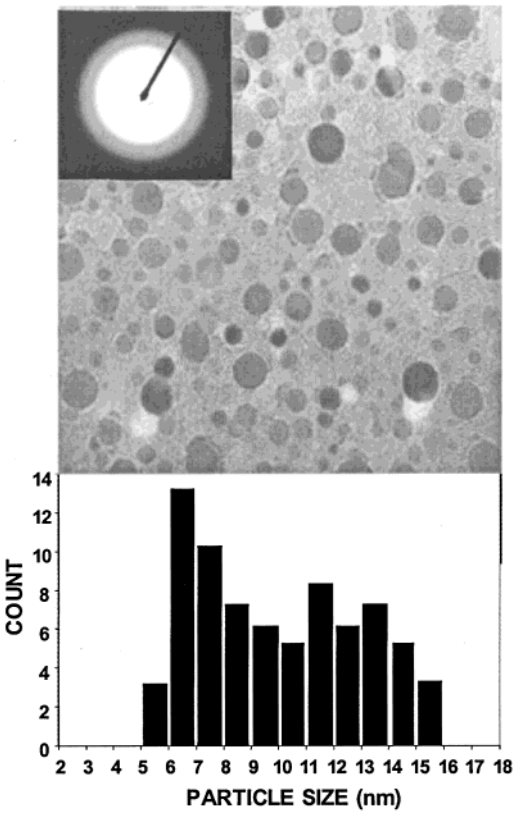

Figure 1. TEM micrograph of 10-undecenoic acid coated amorphous Fe_2O_3 colloidal particles after floating at the air−water interface of a Langmuir trough and being transferred to a copper grid. The inset shows the SAED pattern. Particle size distribution is given below the image.

Magnetic data of the evaporated samples were obtained with Princeton Applied Research vibrating sample magnetometer model 155 (VSM) and a Quantum Design SQUID MPMS-XL (ac and dc modes and maximum static field of ±5 T). The electron paramagnetic resonance (EPR), both at room temperature and at variable temperatures, was recorded on a Bruker EPR ESP 380E spectrometer. For thermal analysis, the samples were heated to 900 °C at a rate of 10° per minute, under a nitrogen atmosphere on a TA 2950 Hi Res TGA.

Figure 1 shows a TEM bright field image of 10-undecenoic acid coated amorphous Fe_2O_3 colloidal particles after floating at the air−water interface of a Langmuir trough and being transferred to a copper grid (the marker represents 10 nm). The near spherical nature of the Fe_2O_3 nanoparticles, 5−16 nm in diameter, can be clearly visualized. All other functionalized nanoparticle samples showed similar shape, size, and size distribution and had electron diffraction patterns showing diffuse rings characteristic of amorphous materials (see inset in Figure 1 showing selected area electron diffraction (SAED) pattern).

FTIR spectra (Figure 2) indicate that the surfactants are bonded to the Fe_2O_3 nanoparticles via ionic bonds, that is, as undecenoate, dodecyl sulfonate, and octyl phosphonate. Thus, in all cases the coating is achieved by a reaction of an acid with Fe_2O_3, which results in the formation of the corresponding Fe^{3+} salts. In the case of the carboxylate headgroup, the C=O stretching mode is

(15) Koltypin, Yu.; Katabi, G.; Cao, X.; Prozorov, R.; Gedanken, A. *J. Non-Cryst. Solids* **1996**, *201*, 159.
(16) Shafi, K. V. P. M.; Gedanken, A.; Goldfarb, R. B.; Felner, I. *J. Appl. Phys.* **1997**, *81*, 6901.
(17) Cao, X.; Koltypin, Yu.; Prozorov, R.; Felner, I.; Gedanken, A. *J. Mater. Chem.* **1997**, *7*, 1007.
(18) Shafi, K. V. P. M.; Gedanken, A.; Prozorov, R.; Balogh, J. *Chem. Mater.* **1998**, *10*, 3445.
(19) Koltypin, Yu.; Cao, X.; Prozorov, R.; Balogh, J.; Kaptas, D.; Gedanken, A. *J. Mater. Chem.* **1997**, *7*, 2453.
(20) Kataby, G.; Prozorov, T.; Koltypin, Yu.; Sukenik, C. N.; Ulman, A.; Gedanken, A. *Langmuir* **1997**, *13*, 6151.
(21) Kataby, G.; Ulman, A.; Prozorov, R.; Gedanken, A. *Langmuir* **1998**, *14*, 1512.
(22) Kataby, G.; Cojocaru, M.; Prozorov, R.; Gedanken, A. *Langmuir* **1999**, *15*, 1703.
(23) Rozenfeld, O.; Koltypin, Y.; Bamnolker, H.; Margel, S.; Gedanken, A. *Langmuir* **1994**, *10*, 627.
(24) Shafi, K. V. P. M.; Gedanken, A.; Prozorov, R. *Adv. Mater.* **1998**, *10*, 590.
(25) Suslick, K. S.; Fang, M.; Hyeon, T. *J. Am. Chem. Soc.* **1996**, *118*, 11960.

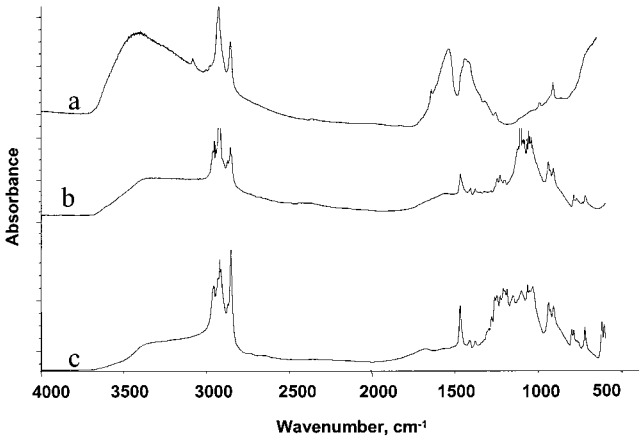

Figure 2. IR spectra of Fe_2O_3 coated with various surfactants: (a) 10-undecenoic acid, (b) octyl phosphonic acid, and (c) dodecyl sulfonic acid.

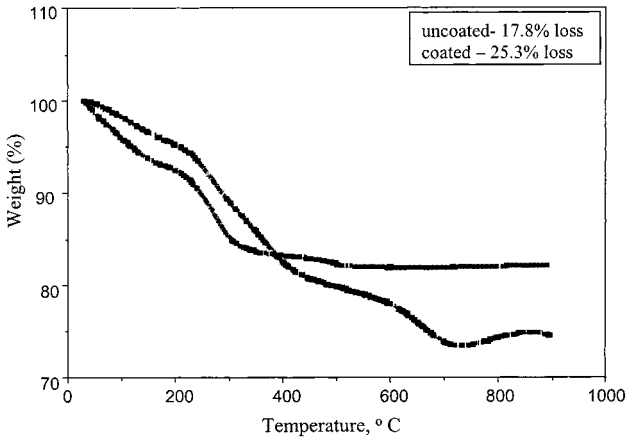

Figure 3. Thermograms of the amorphous Fe_2O_3 nanoparticles: uncoated (gray line) and coated with undecenoic acid (black line).

observed at 1538 and 1441 cm^{-1}, similar to 1539 and 1440 cm^{-1} reported earlier for iron nanoparticles coated by carboxylic acids.[22] The absence of the C═O stretch at 1710 cm^{-1}, common to all carboxylic acids,[26] indicates the binding of a carboxylate to Fe^{3+} ions on the nanoparticle surface. When considering the surface carboxylate bonding, two binding modes have been reported. In the first (e.g., stearic acid on silver surfaces[27]), the carboxylate is bonded symmetrically to the surface and only the symmetrical C═O stretching band appears at 1404 cm^{-1}. In the second (e.g., various carboxylic acids deposited on Cu[28]), the carboxylate is connected to the surface through one oxygen atom, and both the symmetric C═O stretching (1441 cm^{-1}) and the asymmetric stretching (1557 cm^{-1}) were observed, similar to the observations for 11-undecenoate coated Fe_2O_3 nanoparticles. Therefore, our conclusion is that the carboxylate might be connected to the Fe_2O_3 nanoparticle surface through one oxygen atom.

For dodecyl sulfonate coated nanoparticles, the RSO_3^- asymmetric and symmetric stretching vibrations at 1225−1177 and 1062 cm^{-1}, respectively, confirm the bonding of the sulfonic acids to the Fe_2O_3 nanoparticle surfaces via ionic bonds. The CH_2 scissoring motion (δ) at 1468 cm^{-1} is typical of an all-trans methylene chain (~1467 cm^{-1}),[26] suggesting that the alkyl chain is long enough to organize in an ordered assembly. This is similar to the findings in self-assembled monolayers of dodecanethiol ($CH_3(CH_2)_{11}$-SH) on gold surfaces.[29,30] For the octyl phosphonate functionalized Fe_2O_3 nanoparticles, the P═O stretching band appears at 1231 cm^{-1}, an indication that the phosphonate group is connected to the Fe_2O_3 surface by ionic bonds. As in the case of the dodecyl sulfonate, a sharp band at 1468 cm^{-1} indicates an all-trans conformation and an ordered assembly.

In the case of the undecenoate-coated Fe_2O_3 nanoparticles, the strong absorption bands in the CH_2 stretching region, 2928 cm^{-1} (asymmetric) and 2853 cm^{-1} (symmetric), clearly indicate the presence of the surfactant chains on the nanoparticle surface. Furthermore, the presence of the vinylic hydrogens at 3080 cm^{-1} confirms that the terminal double bonds were not altered during the sonochemical reaction. Taken together, the infrared data suggest that the adsorbed undecenoate molecules are significantly disordered. This is not surprising, given the length of the alkyl chain (C_{11}) and the terminal double bond, which introduces disorder to the assembly.

For the asymmetric and symmetric C−H stretching region at 3000−2800 cm^{-1}, the sulfonate-coated nanoparticles show values of 2958 cm^{-1} for $\nu_{as}(CH_3)$, 2919 cm^{-1} for $\nu_{as}(CH_2)$, 2873 cm^{-1} for $\nu_s(CH_3)$, and 2852 cm^{-1} for $\nu_s(CH_2)$. The FTIR spectrum of the phosphonate-coated nanoparticles shows values of 2956 cm^{-1} for $\nu_{as}(CH_3)$, 2915 cm^{-1} for $\nu_{as}(CH_2)$, 2872 cm^{-1} for $\nu_s(CH_3)$, and 2851 cm^{-1} for $\nu_s(CH_2)$. The above values suggest that for these functionalized Fe_2O_3 nanoparticles, the alkyl chains are ordered, although the peak positions do not indicate a close-packed, solidlike arrangement, as reported earlier.[20] Hostetler and co-workers have studied alkanethiolate-functionalized gold nanoparticles using infrared spectroscopy.[31] For the $C_{16}H_{33}S$-functionalized gold nanoparticles, they reported 2954 cm^{-1} for $\nu_{as}(CH_3)$, 2918 cm^{-1} for $\nu_{as}(CH_2)$, 2873 cm^{-1} for $\nu_s(CH_3)$, and 2848 cm^{-1} for $\nu_s(CH_2)$. They noted that a crystalline microenvironment is seen for alkyl chains C_6 or greater, as is evident by the above CH_2 stretches ($\nu_s(CH_2)$ and $\nu_{as}(CH_2)$).

The thermograms of the amorphous Fe_2O_3 samples with and without undecenoate are shown in Figure 3. The mass loss, as well as the high desorption temperature, confirms strong ionic binding between the carboxylate and the Fe_2O_3 nanoparticles. The net weight loss of the undecenoic acid coated Fe_2O_3 samples is 7.5%, indicating, after accounting for the weight loss for uncoated Fe_2O_3 particles (17.8%), a full surface coverage of Fe_2O_3 nanoparticles of average size 5−16 nm.

The magnetization curves of the amorphous Fe_2O_3 and the surfactant-coated nanoparticles, measured at room temperature, are presented in Figure 4. Figure 5 exhibits zero-field cooled and field cooled (ZFC and FC) curves for the amorphous Fe_2O_3 nanoparticles. The data show no hysteresis and no saturation up to a magnetic field of 18 kG (Figure 4), indicating that the as-prepared amorphous particles are superparamagnetic. Zero-field cooled and field cooled studies (Figure 5) further indicate that these superparamagnetic nanoparticles behave like spin glasses, which is characteristic of amorphous nanoparticles.[32] The

(26) Bellamy, L. J. *The Infrared Spectra of Complex Molecules*; Chapman and Hall: New York, 1986.
(27) Ahn, S. J.; Son, D. H.; Kim, K. *J. Mol. Struct.* **1994**, *324*, 223.
(28) Tao, Y.-T. *J. Am. Chem. Soc.* **1993**, *115*, 4350.
(29) For reviews on self-assembled monolayers, see: (a) Ulman, A. *An Introduction to Ultrathin Organic Films*; Academic Press: Boston, 1991. (b) Ulman, A. Formation and Structure of Self-Assembled Monolayers. *Chem. Rev.* **1996**, *96*, 1533. (c) Bishop, A.; Nuzzo, R. G. *Curr. Opin. Colloid Interface Sci.* **1998**, *1*, 127.
(30) For a review on SAMs on thiols, see: *Thin Films*; Ulman, A., Ed.; Academic Press: Boston, 1999; Volume 23.
(31) Hostetler, M. J.; Stokes, J. J.; Murray, R. W. *Langmuir* **1996**, *12*, 3604.

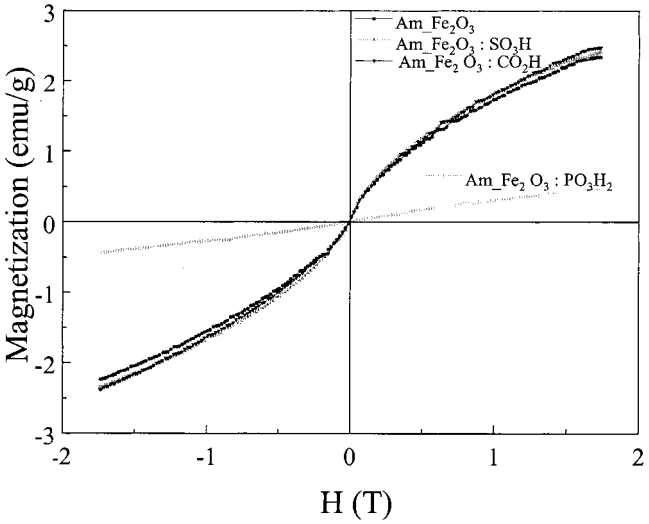

Figure 4. Room-temperature magnetization curves of as-prepared and surfactant-coated amorphous Fe_2O_3 nanoparticles.

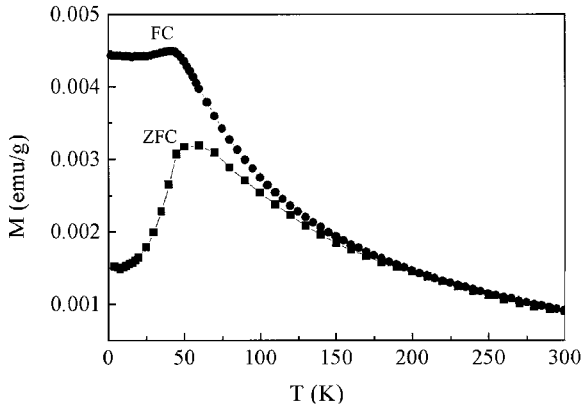

Figure 5. Zero-field cooled and field cooled (ZFC and FC) magnetic curves of the as-prepared amorphous Fe_2O_3 nanoparticles, measured in a dc field of 2 Oe.

average blocking temperature is about 60 K. The separation of the ZFC and FC curves (far from the maximum TB_{max}) is due to size distribution of the particles. Surprisingly, the phosphonate-coated nanoparticles behave in a strikingly different manner from those with other surfactants. The data show a very low value in magnetization with a constant magnetization increment. One possible reason may be that the size of these nanoparticles is significantly different from that of the other functionalized samples. However, TEM images do not support this explanation.

To further investigate the anomalous behavior of the phosphonate-coated Fe_2O_3 nanoparticles, we carried out detailed EPR studies. Again, the phosphonate-coated nanoparticles stand out in their behavior. For all nanoparticles, except for the phosphonate-coated, an increase in peak-to-peak line width (ΔH_{pp}) is observed with decreasing temperature **(**Figures 6 and 7B), with a linewidth of about 1800−2000 G at 140 K. This is a typical behavior of superparamagnetic particles. Magnetic crystalline anisotropy, in conjunction with the random orientations of the particles, causes line broadening in the ferromagnetic resonance (FMR) spectra of the monodomain ferromagnetic particles.[16,33] However, for superparamagnetic nanoparticles, whose direction of magnetization fluctuates at a rate faster than the Larmor frequency, this results in a narrow resonance line, due to an averaging effect of this fluctuation on the magnetocrystalline anisotropy. On lowering the temperature, the resonance line of the superparamagnetic particle broadens as the averaging effect of thermal fluctuations is reduced and the direction of magnetization is blocked, at first in bigger and progressively in smaller particles. Thus, the narrow resonance line at room temperature, which progressively broadens on lowering the temperature, confirms the superparamagnetic character of the amorphous Fe_2O_3, as well as the undecenoate- and sulfonate-coated samples, as noticed earlier by magnetic studies. The effective g-value of 2.04 is in good agreement with that reported for Fe_2O_3.[34] The spectrum of the Fe^{3+} coupled pair ($Fe^{3+}-O-Fe^{3+}$) in Fe_2O_3 gives a resonance line at $g_{eff} = 2.0$. A weak signal is also observed at about $g = 4.28$,

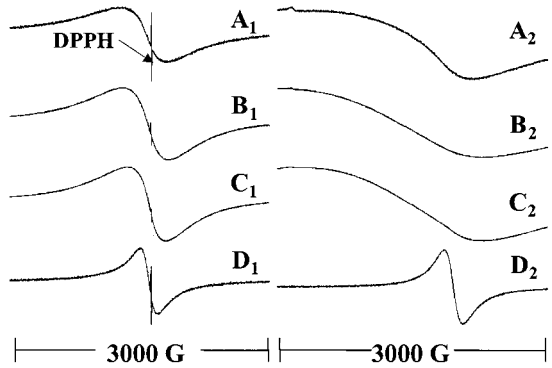

Figure 6. EPR spectra (X-band) of amorphous Fe_2O_3 nanoparticles coated with different acids at (1) room temperature and (2) 140 K: (A) Am Fe_2O_3; (B) Am Fe_2O_3 + CH_2=$CH(CH_2)_8$-COOH; (C) Am Fe_2O_3 + $C_{12}H_{23}SO_3H$, and (D) Am Fe_2O_3 + C_8H_{17}-PO_3H_2.

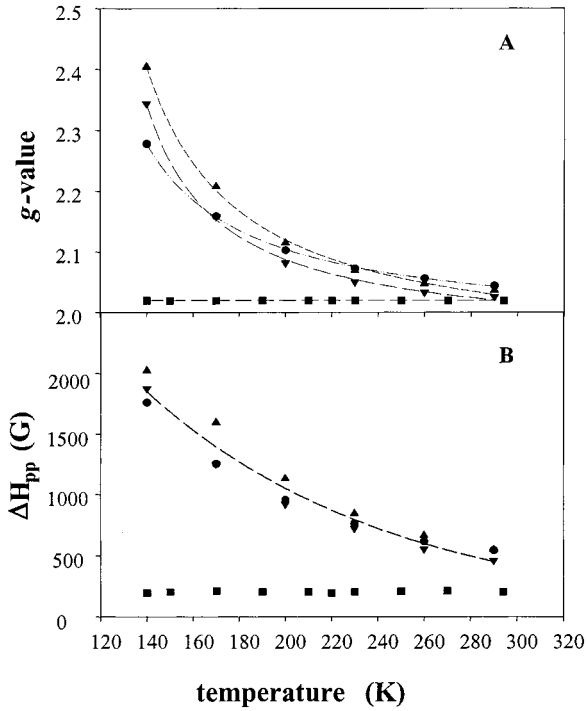

Figure 7. Nanoparticle g-value (A) and EPR line width (ΔH_{pp}) (B) dependence on temperature: (▲) Am Fe_2O_3, (▼) Am Fe_2O_3 + CH_2=$CH(CH_2)_8COOH$, (●) Am Fe_2O_3 + $C_{12}H_{23}SO_3H$, and (■) Am Fe_2O_3 + $C_8H_{17}PO_3H_2$. The dashed line in (B) represents average line widths of the Am Fe_2O_3, Am Fe_2O_3 + CH_2=CH-$(CH_2)_8COOH$, and Am Fe_2O_3 + $C_{12}H_{23}SO_3H$.

(32) Morup, S. *Europhys. Lett.* **1994**, *28*, 671.
(33) Leslie-Pelecky, D. L.; Rieke, R. D. *Chem. Mater.* **1996**, *8*, 1770.

which can be ascribed to an isolated Fe^{3+} in the orthorhombic field.[34] Interestingly, the EPR data of amorphous octyl phosphonate coated Fe_2O_3 nanoparticles show only one signal at $g \sim 2$ with a constant field of resonance (Figure 7A), indicating a possible superantiferromagnetic behavior.[35] All the other three types of nanoparticles show an increase in *g*-value as the temperature is lowered, most likely due to an increase in an internal field.[36]

So far, we have presented ample evidence for the different behavior of phosphonate-coated Fe_2O_3 nanoparticles. As we noted above, TEM does not support the assumption that this behavior results from particles that do not contain the same Fe_2O_3 nanoparticles. That phosphonate coating results in diminished magnetization was observed previously when the coating was carried out *after* the sonochemical synthesis; hence, all coated samples were prepared from the same batch of amorphous Fe_2O_3 nanoparticles.[37] There, we measured the surface area of different coated samples and concluded that the size of amorphous Fe_2O_3 nanoparticles does not change after coating with phosphonate groups, and thus no etching of nanoparticles occurred. Therefore, differences in the magnetization must result from the bonding of the phosphonate groups to the Fe_2O_3 nanoparticle surface and might imply antiferromagnetic coupling[34] which results in superantiferromagnetic nanoparticles.[35] The net magnetization in superantiferromagnetic materials arises mainly from the interaction between unpaired interfacial spins. As a result, the overall magnetization of superantiferromagnetic domains is much lower than superparamagnetic domains.

In simple Fe^{3+} dimers, that is, complexes with two high-spin Fe^{3+} ions bridged by an oxide anion to form an $[Fe_2(\mu\text{-}O)]^{4+}$ unit,[38] there is a relatively strong antiferromagnetic exchange interaction that leads to an appreciable decrease in the $\chi_M T$ value compared to that expected for two noninteracting high-spin Fe^{3+} ions. In such systems, the oxygen bridge mediates a direct antiferromagnetic exchange of all five of the 3d electrons to yield an $S = 0$ ground state. Such direct antiferromagnetic coupling should involve in the present case the phosphorus empty d-orbitals. However, the sulfur atom in the sulfonate-coated nanoparticles also has empty d-orbitals, but the sulfonate-functionalized nanoparticles are similar in magnetic behavior to the undecenoate-functionalized nanoparticles. The only feature that distinguishes the phosphonate is its extra negative charge, as compared to the carboxylate and sulfonate groups, which makes it a bridging bidentate ligand. Hence, our results suggest that monodentate ligands cannot mediate an antiferromagnetic coupling between two *surface* Fe^{3+} ions in amorphous Fe_2O_3 nanoparticles. (This is not the case in bulk materials, where carboxylate ions act as bidentate ligands and facilitate antiferromagnetic coupling, for example, in basic triiron acetate complexes.) Given the discussion above, the conclusion is that both phosphorus empty d-orbitals and oxygen electron pairs must participate in the antiferromagnetic coupling. A possible suggested mechanism might be double superexchange through a $Fe^{3+}-O-P-O-Fe^{3+}$ pathway. At this point, however, we cannot provide theoretical support for any mechanism and remain with the experimental data that show a significant decrease in magnetization due to phosphonate binding.

We presented results of experiments where sonochemical decomposition of $Fe(CO)_5$ was carried out in the presence of different surfactants. The reactions give stable colloids of undecenoate, dodecyl sulfonate, and octyl phosphonate coated Fe_2O_3 nanoparticles of 5−16 nm in diameter. The ionic binding of the surfactants to the nanoparticle surfaces is confirmed by FTIR spectroscopy. EPR measurements, magnetization curves, and zero-field cooled and field cooled studies indicate that the as-prepared amorphous nanoparticles are superparamagnetic. These studies show that the phosphonate-coated nanoparticles behave in a strikingly different manner from the other particles. It is proposed that the extra negative charge on the phosphonate, as compared to the carboxylate and sulfonate groups, makes it a strong bridging bidentate ligand, resulting in the formation of strong ionic bonds to the *surface* Fe^{3+} ions, which decreases the number of unpaired spins possibly through a double superexchange mechanism through a $Fe^{3+}-O-P-O-Fe^{3+}$ pathway.

Acknowledgment. This research was funded by the NSF through the MRSEC for Polymers at Engineered Interfaces. We thank the Polytechnic University for the support of K.V.P.M.S. Support to the FT-EPR/CUNY@SI Facility from the NY State Higher Education Applied Technology Program is acknowledged. The technical assistance of A. Derory is much appreciated. C.E. is grateful to Dr. Vilminot for fruitful discussions. A.U. thanks the Alexander von Humboldt Foundation for supporting his stay in the University of Heidelberg.

LA010421+

(34) Tanaka, K.; Kamiya, K.; Yoko, T.; Tanabe, S.; Hirao, K.; Soga, N. *J. Non-Cryst. Solids* **1989**, *109*, 289.

(35) Tolbert, S. H.; Sieger, P.; Stucky, G. D.; Aubin, S. M. J.; Wu, C.-C.; Hendrickson, D. N. *J. Am. Chem. Soc.* **1997**, *119*, 8652.

(36) Oseroff, S. B. *Phys. Rev. B* **1982**, *25*, 6584.

(37) Yee, C.; Kataby, G.; Ulman, A.; Prozorov, T.; White, H.; King, A.; Rafailovich, M.; Sokolov, J.; Gedanken, A. *Langmuir* **1999**, *15*, 7111.

(38) (a) Murray, K. S. *Coord. Chem. Rev.* **1974**, *12*, 1. (b) Ou, C. C.; Wollman, R. G.; Hendrickson, D. N.; Potenza, J. A. *J. Am. Chem. Soc.* **1978**, *100*, 4717. (c) Gomez-Romero, P.; Witten, E. H.; Reiff, W. M.; Jameson, G. B. *Inorg. Chem.* **1990**, *29*, 5211.